

A natural variant and an engineered mutation in a GPCR promote DEET resistance in *C. elegans*

Emily J. Dennis¹, Xin Jin^{2,*}, May Dobosiewicz², Laura B. Duvall¹, Philip S. Hartman³, Cornelia I. Bargmann^{2,4}, & Leslie B. Vosshall^{1,4,5}

DEET (*N,N*-diethyl-*meta*-toluamide) is a synthetic chemical, identified by the United States Department of Agriculture in 1946 in a screen for repellents to protect soldiers from mosquito-borne diseases^{1,2}. Since its discovery, DEET has become the world's most widely used arthropod repellent³, and is effective against many invertebrates, including biting flies⁴, honeybees⁵, ticks⁶, and land leeches^{4,7}. In insects, DEET acts on the olfactory system^{5,8-14} and requires the olfactory receptor co-receptor *orco*^{9,11-13}, but its specific mechanism of action remains controversial. Here we show that the nematode *Caenorhabditis elegans* is sensitive to DEET, and use this genetically-tractable animal to test repellent hypotheses from insects to understand how this synthetic compound is able to affect the behaviour of invertebrates separated by millions of years of evolution. We found that DEET is not a volatile repellent, but interfered selectively with chemotaxis to a variety of attractant and repellent molecules, and induced pausing to disrupt chemotaxis to some odours but not others. In a forward genetic screen for DEET-resistant animals, we identified a single G-protein-coupled receptor, *str-217*, which is expressed in a single pair of DEET-responsive chemosensory neurons, ADL. Both engineered *str-217* mutants and a wild isolate of *C. elegans* carrying a deletion in *str-217* are DEET-resistant. DEET interferes with behaviour in an odour-selective manner by inducing an increase in average pause length during chemotaxis and exploration, and this increase in pausing requires both *str-217* and ADL neurons. Finally, we found that ADL neurons are activated by DEET and that optogenetic activation of ADL increased average pause length. This is consistent with the “confusant” hypothesis, in which DEET is not a simple repellent but modulates multiple olfactory pathways to scramble the behavioural response to otherwise attractive stimuli^{12,13}. Our results suggest a consistent motif for the effectiveness of DEET across widely divergent taxa: an effect on multiple chemosensory neurons to disrupt the pairing between odorant stimulus and behavioural response.

We used standard chemotaxis assays¹⁵⁻¹⁷ (Fig. 1a) to explore whether and how *C. elegans* nematodes respond to DEET. There are currently three competing hypotheses about the mechanism of DEET based on work in insects: “Smell-and-repel” —DEET is detected by olfactory pathways that trigger avoidance^{5,10,14,18}, “masking” —DEET selectively blocks olfactory pathways that mediate attraction⁸⁻¹⁰, and “confusant” —DEET modulates multiple olfactory sensory neurons to scramble the perception of an otherwise attractive stimulus^{12,13}. Inspired

by these hypotheses, we tested how DEET may interfere with olfactory behaviours in nematodes to identify similarities and differences with work in insects.

To test the smell-and-repel hypothesis, we presented DEET as a volatile point source. DEET was not repellent alone (Fig. 1b), similar to previous results in *Drosophila melanogaster* flies⁹ and *Aedes aegypti* mosquitoes¹³. To address the possibility that DEET could be masking responses to attractive odorants^{8,9} or directly inhibit-

¹Laboratory of Neurogenetics and Behaviour, The Rockefeller University, New York, NY 10065, USA

²Lulu and Anthony Wang Laboratory of Neural Circuits and Behaviour, The Rockefeller University, New York, NY 10065, USA

³Department of Biology, Texas Christian University, Fort Worth, TX 76129, USA

⁴Kavli Neural Systems Institute

⁵Howard Hughes Medical Institute

*Current address Society of Fellows, Harvard University, Cambridge, MA 02138

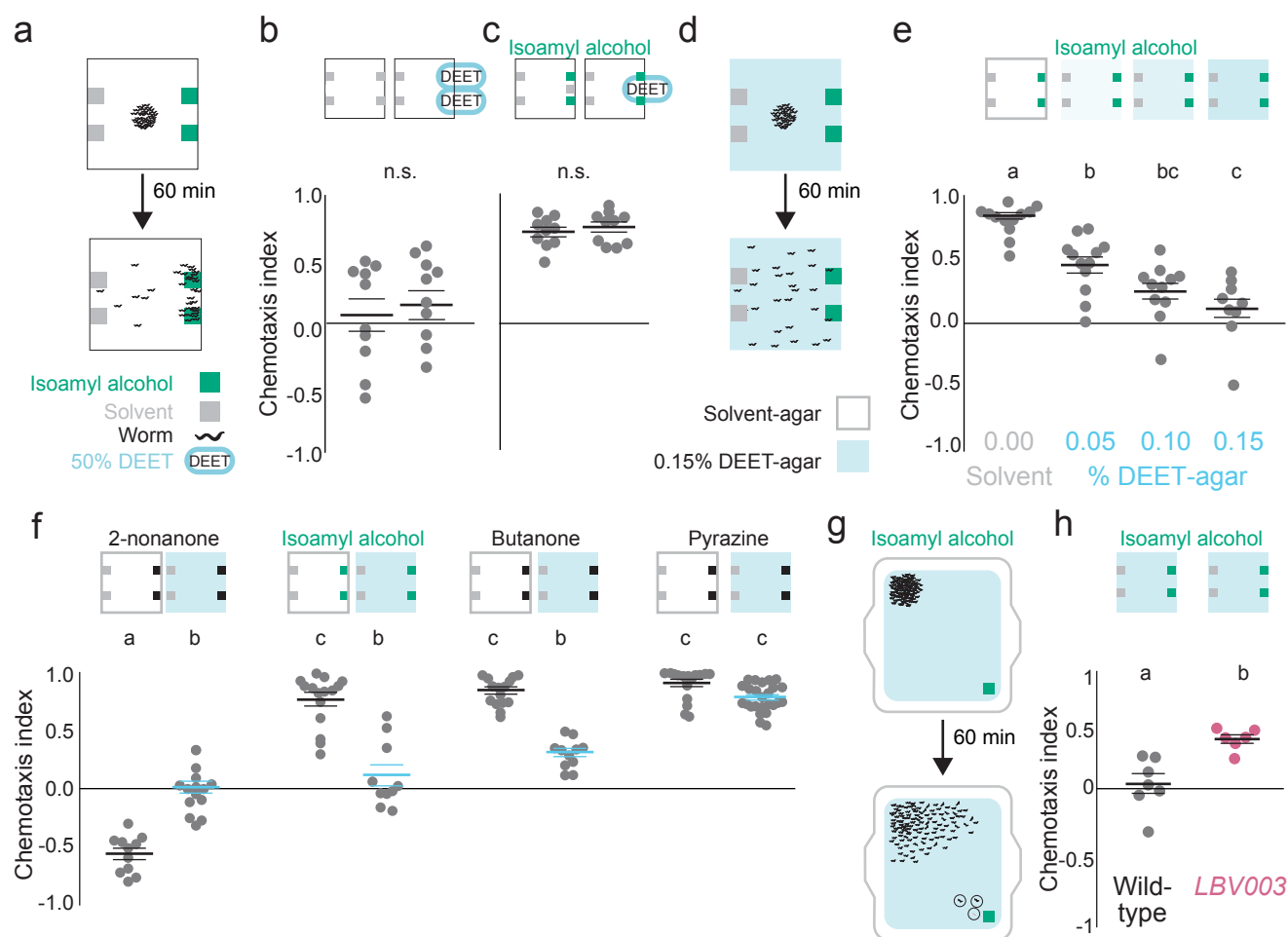


Figure 1 | DEET interferes with *C. elegans* chemotaxis **a**, Schematic of chemotaxis assay. **b-c**, Chemotaxis of wild-type animals with point source stimuli of DEET alone (**b**) or DEET with isoamyl alcohol (**c**) (N=10). **d**, Schematic of chemotaxis assay on DEET-agar plates. **e**, Wild-type chemotaxis to isoamyl alcohol on DEET-agar plates of the indicated concentrations (N=10-13). **f**, Chemotaxis of wild-type animals on solvent-agar (grey) or DEET-agar (blue) in response to the indicated odorants (N=11-24). **g**, Schematic of forward genetic screen with hypothetical DEET-resistant mutants circled. **h**, Chemotaxis of wild-type (grey) and *LBV003* mutant (pink) animals (N=6-7). For all plots, each dot represents a chemotaxis index of a single population assay (50-250 animals). Horizontal lines indicate mean \pm s.e.m. Data labelled with different letters indicate significant differences ($p < 0.05$, Student's T-test (**b** and **h**) or one-way (**e**) or two-way (**f**) ANOVA and Tukey's Post-hoc test).

ing their volatility¹⁰, we presented DEET alongside the attractant isoamyl alcohol, both as point sources, and found that it had no effect on attraction (Fig. 1c). In considering alternate ways to present DEET, we mixed low doses of DEET uniformly into the chemotaxis agar and presented isoamyl alcohol as a point source (Fig. 1d). In this configuration, DEET-agar reduced chemotaxis to isoamyl alcohol in a dose-dependent manner (Fig. 1e). To ask if DEET has a general effect on chemotaxis, we tested two additional attractants, butanone and pyrazine,

as well as the volatile repellent 2-nonanone. Behavioural responses to butanone requires the same pair of primary sensory neurons as isoamyl alcohol (AWC), while pyrazine and 2-nonanone require two different pairs of primary sensory neurons (AWA and AWB, respectively)^{16,19}. DEET eliminated both attraction to butanone and avoidance of 2-nonane, indicating that it can affect responses to both positive and negative chemosensory stimuli (Fig. 1f). In contrast, DEET-agar had no effect on chemotaxis toward the attractant pyrazine (Fig. 1f). We conclude that

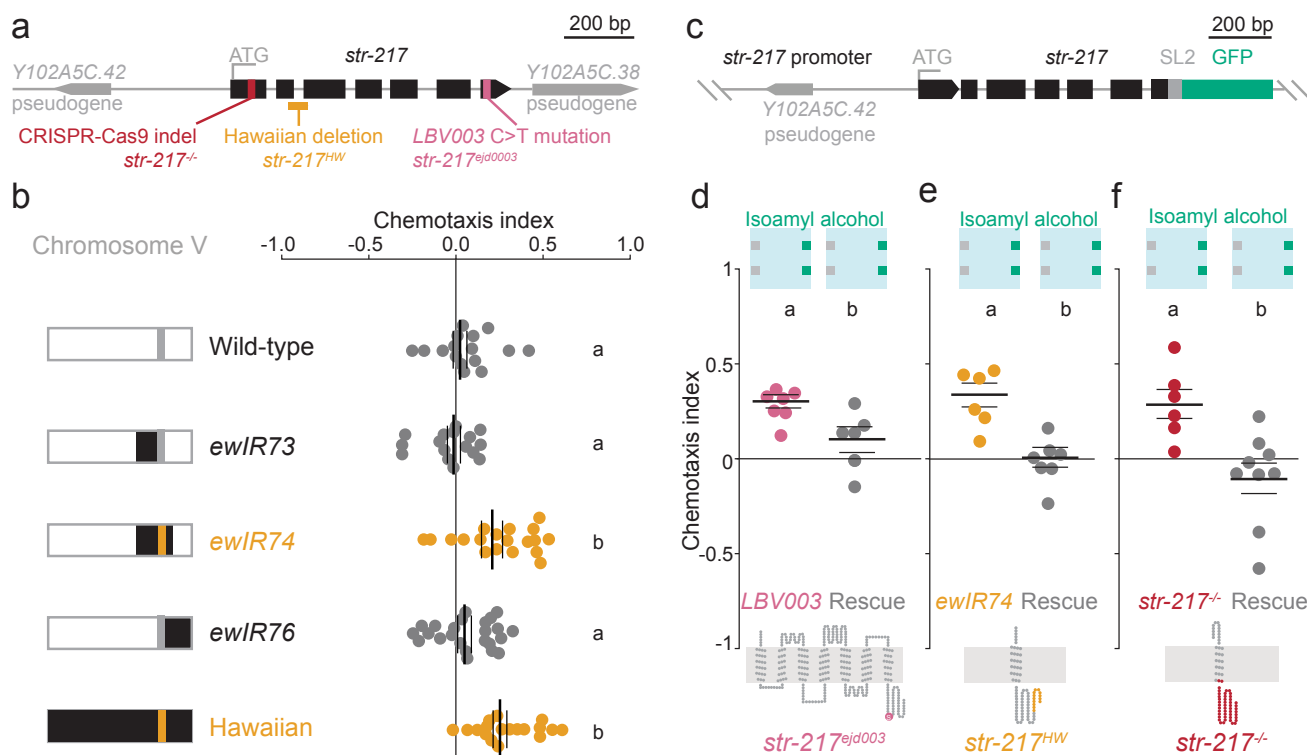


Figure 2 | *str-217* mutants are DEET-resistant. **a**, *str-217* genomic locus. **b**, Left: schematic of chromosome V in each strain: wild-type (white), Hawaiian (black), *str-217^{+/+}* (grey), *str-217^{HW}* (orange). Right: chemotaxis of the indicated strain (N=16-24). **c**, Schematic of *str-217* rescue construct. **d-f**, Chemotaxis indices of the indicated strains (N=6-9). Predicted *str-217* protein topology of each mutant is indicated below each plot. In **b**, **d-f** each dot represents a chemotaxis index of a single population assay (50-250 animals). Horizontal lines indicate mean \pm s.e.m. Data labelled with different letters indicate significant differences ($p < 0.05$ ANOVA and Tukey's Post-hoc test in **b**, and two-sided Student's t-test in **d-f**).

DEET chemosensory interference is odour-selective, can affect both attractive and repulsive stimuli, and is not a result of non-specific or toxic effects of DEET.

Identifying genes required for DEET-sensation has been of interest for some time. A forward genetic approach in *Drosophila melanogaster* flies yielded an X-linked DEET-insensitive mutant²⁰ and a population genetics approach in mosquitoes identified a dominant genetic basis for DEET-insensitivity²¹, but neither study identified the genes underlying these changes. Reverse genetic experiments in *Drosophila* flies and three mosquito species have identified the insect odorant receptors as a molecular target of DEET^{9,11-14}. However, this chemosensory gene family is not found outside of insects^{22,23},

raising the question of what pathways are required for DEET-sensitivity in non-insect invertebrates. To gain insights into the mechanisms of DEET repellency in *C. elegans*, we carried out a forward genetic screen for mutants capable of chemotaxing toward isoamyl alcohol on DEET-agar plates (Fig. 1g). We obtained 5 DEET-resistant animals, three of which produced offspring that consistently chemotaxed toward isoamyl alcohol on DEET-agar plates (Fig. 1h, and data not shown). Whole genome sequencing allowed us to identify candidate causal mutations in these 3 strains²⁴, and we chose to focus on *LBV003*, which maps to *str-217*, a predicted G protein-coupled receptor (Fig. 2a). In the course of mapping *str-217*, we discovered that a divergent strain of *C. elegans* isolated in Hawaii, CB4856 (Hawaiian),

is naturally resistant to DEET (Fig. 2b). This Hawaiian strain contains a 138-base pair deletion in *str-217* (*str-217^{HW}*) that affects exons 2 and 3 and an intervening intron, leading to a mutant strain with a predicted frame shift indel and early stop codon (Fig. 2a). To confirm that DEET resistance maps to *str-217^{HW}*, we tested three near-isogenic lines with a single, homozygous genomic segment of Hawaiian chromosome V introgressed into a wild-type (Bristol N2) background²⁵ (Fig. 2b). Only the ewIR74 line contains *str-217^{HW}* and, like the parent Hawaiian strain, is DEET-resistant (Fig. 2b). To provide further confirmation that *str-217* is required for DEET sensitivity in these strains, we generated two additional genetic tools: an engineered predicted null mutant produced by CRISPR-Cas9 genome-editing (*str-217^{-/-}*) (Fig. 2a), and a rescue/reporter plasmid that expresses both wild-type *str-217* and green fluorescent protein (GFP) under control of the predicted *str-217* promoter (Fig. 2c). The LBV003 strain (Fig. 2d), Hawaiian introgressed strain ewIR74 (Fig. 2e), and the *str-217^{-/-}* engineered mutant strain (Fig. 2f) all showed chemotaxis on DEET-agar (Fig. 2d-f). Expression of the *str-217* rescue/reporter construct in these three strains rendered all three DEET-resistant mutants fully sensitive to DEET, in that none chemotaxed to isoamyl alcohol on DEET-agar (Fig. 2d-f).

We next turned to the neuronal mechanism by which DEET disrupts chemotaxis in *C. elegans*. In insects, DEET interacts directly with chemosensory neurons and the odorant receptors that they express^{9,11-14}. Isoamyl alcohol is primarily sensed by the AWC chemosensory neuron¹⁹. To ask if DEET modulates primary sensory detection of isoamyl alcohol, we used *in vivo* calcium imaging to monitor AWC activity in the presence and absence of DEET. AWC responded to the addition of DEET with a rapid increase in calcium that decreased to baseline over the course of 11 min of chronic DEET stimulation (Extended Data Fig. 1a). In the presence of

DEET, AWC responses to isoamyl alcohol decreased in magnitude, but there was no observed difference in AWC activity between wild-type and *str-217^{-/-}* mutants in the presence or absence of DEET (Extended Data Fig. 1b-c). This suggests that AWC sensory neurons are not the primary functional target of DEET.

To identify the functionally relevant neurons, we determined where *str-217* is expressed by examining the *str-217* rescue/reporter strain, and found GFP expression in a single pair of chemosensory neurons, called ADL (Fig. 3a). ADL is not required for chemotaxis to isoamyl alcohol, suggesting an indirect role for ADL in DEET chemosensory interference²⁶. To ask if ADL neuronal function is required for DEET-sensitivity, we expressed tetanus toxin light chain, which inhibits chemical synaptic transmission by cleaving the synaptic vesicle protein synaptobrevin, in ADL^{27,28}. These animals showed the same level of DEET-resistance as *str-217* mutants (Fig. 3b). Since both *str-217* and ADL function are required for DEET-sensitivity, we used calcium imaging to ask if ADL responds to DEET, and if this requires *str-217* (Fig. 3c). Both wild-type and *str-217^{-/-}* mutants carrying the rescue/reporter plasmid, but not *str-217^{-/-}* mutants, showed calcium responses to DEET (Fig. 3d-e, h). In control experiments, we showed that the known ADL agonist, the pheromone C9 (ref. ²⁷), activated ADL in both wild-type and *str-217^{-/-}* mutant animals (Fig. 3f-h). This suggests that the *str-217^{-/-}* mutation has a selective effect on ADL function. From these data, we conclude that disrupting either ADL activity or *str-217* is sufficient to confer DEET-resistance in *C. elegans*. We note that neither *str-217* mutants nor ADL-deficient animals return fully to wild-type levels of chemotaxis (Fig. 3b), suggesting that additional genes and neurons contribute to DEET sensitivity in *C. elegans*. To ask if *str-217* is a direct molecular target of DEET, we carried out calcium imaging experiments in HEK293T cells. DEET did not activate HEK293T cells expressing *str-217* (Extended

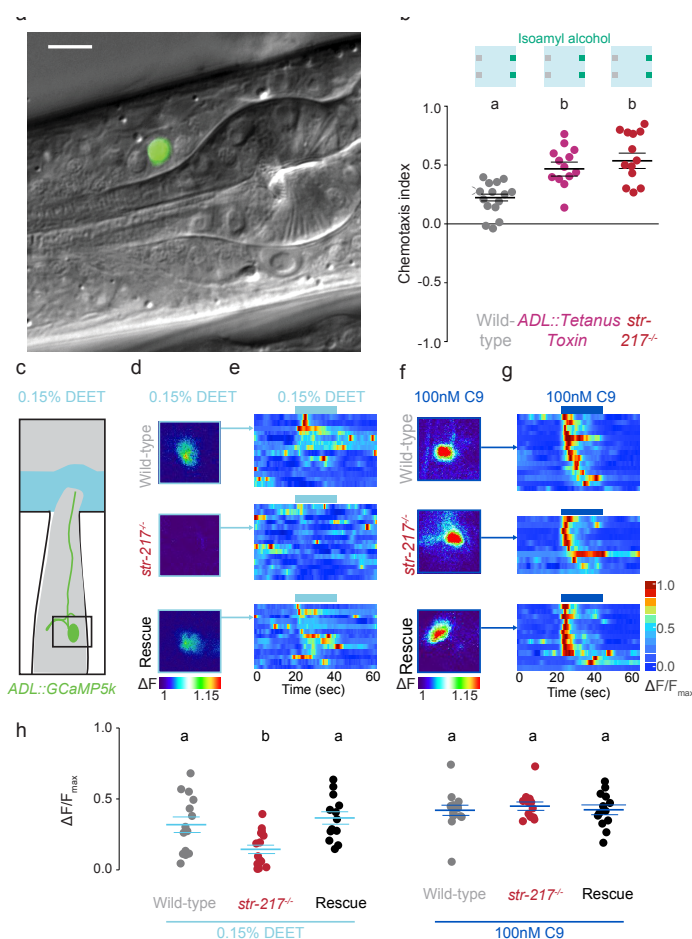


Figure 3 | *str-217* is expressed in ADL, a DEET-responsive chemosensory neuron required for DEET-sensitivity. **a**, GFP expression in a single ADL neuron from *str-217* rescue/reporter construct (scale bar: 10 μ m). **b**, Chemotaxis of the indicated strains. **c**, Schematic of microfluidic calcium imaging assay. **d**, Pseudocolored images of ADL response to 0.15% DEET in animals of the indicated genotype (increase in mean fluorescence 20 sec after the first DEET pulse minus mean of 20 sec before the 0.15% DEET pulse). **e**, Heat maps of calcium imaging data in response to 0.15% DEET. Each row represents ADL imaged in one animal, cropped to show only the first pulse. **f**, Pseudocolored images of ADL response to 100 nM C9 pheromone in animals of the indicated genotype calculated as in d. **g**, Heat maps of calcium imaging data in response to 100 nM C9 pheromone. Each row represents ADL imaged in one animal, cropped to show only the first pulse. **h**, Mean normalized ADL calcium responses during the first DEET or C9 pulse in animals of the indicated genotype from data in e and g. In b and h, horizontal lines represent mean \pm s.e.m. In b, each dot represents a single population assay and in h, each dot represents a single neuron in a single animal. Data labelled with different letters indicate significant differences ($p < 0.05$, one-way (b) or two-way (h) ANOVA and Tukey's Post-hoc test).

Data Fig. 2), although we cannot exclude the possibility that this nematode receptor is non-functional in mammalian tissue culture cells. It is also possible that *str-217* is not the direct *in vivo* target of DEET, but is involved indirectly in signalling or modulation of DEET-specific responses in ADL.

We next explored how ADL activity can interfere with chemotaxis. Population chemotaxis assays report the location of the animal at the end of the experiment, and do not reveal the details of navigation strategy. To investigate which aspects of chemotaxis are affected by DEET, we tracked the position and posture of individual animals on DEET-agar or solvent-agar plates (Fig. 4a-g). Wild-type, but not *str-217*^{-/-} mutant animals (Fig. 4d), showed a dramatic increase in average pause length on DEET-agar. To determine if the increase in average pause length occurs only in the context of chemotaxis to isoamyl alcohol, or

as a consequence of DEET alone, we tracked wild-type, *str-217*^{-/-} mutant (Fig. 4e), and ADL::Tetanus toxin (Fig. 4f) animals on DEET-agar and solvent-agar plates with no additional odorants. Only wild-type animals had a higher average pause length on DEET-agar (Fig. 4e-f). Average pause length was unaffected by DEET in *str-217*^{-/-} and ADL::Tetanus toxin animals (Fig. 4e-f). Consistent with our prior observation that chemotaxis to pyrazine was unaffected by DEET, wild-type animals showed no increase in average pause length when chemotaxing to pyrazine on DEET-agar (Fig. 4g). This suggests the interesting possibility that pyrazine chemotaxis is not only *str-217*- and ADL-independent, but can overcome the effect of DEET on average pause length. To test if ADL activity alone is sufficient to increase average pause length, we carried out an optogenetic experiment by expressing the light-sensitive ion channel ReaChR²⁹ in ADL in wild-type animals, and tracking locomotor behaviour on chemotaxis plates. We

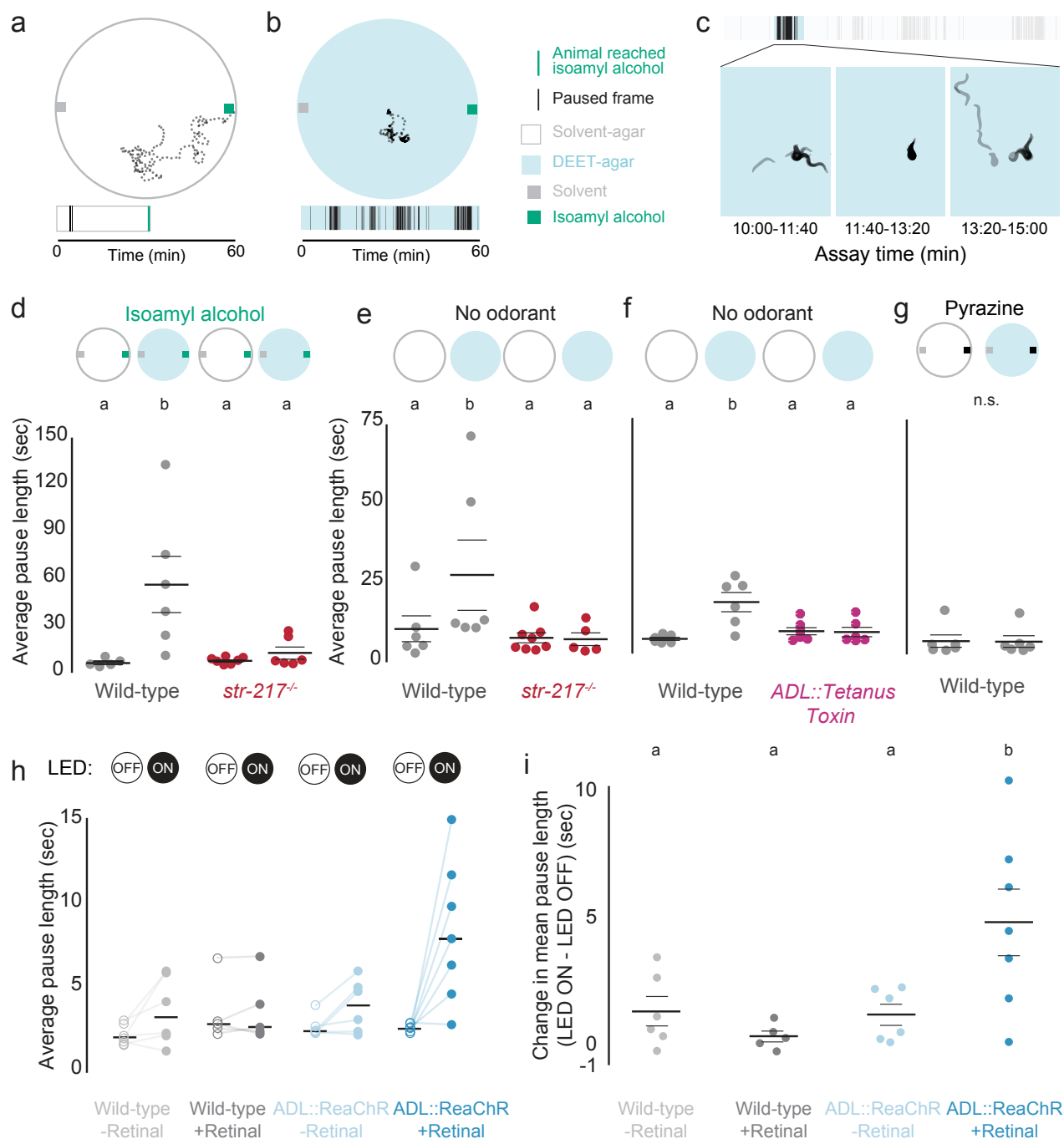


Figure 4 | DEET increases average pause length through *str-217* and ADL. **a-b**, Top: example trajectories of a single wild-type animal chemotaxing to isoamyl alcohol on solvent-agar (a) or a different animal on DEET-agar (b) plate. Each dot depicts the x, y position of a single animal once every 10 sec. Bottom: raster plots indicating paused frames for each animal depicted above. **c**, Example pauses from the tracked animal in b. Images were extracted every 18 frames (6 sec), cropped, and made into a silhouette. 16 silhouettes were overlaid to create each snapshot of activity. **d-g**, Average pause length for each experiment on plates with the indicated stimuli and genotypes (N=6-7 plates, 4-15 animals per plate). **h**, Average pause length of the indicated genotype with LED off (open circles) or on (closed circles), with lines connecting each experimental pair. **i**, Difference in average pause length for each experiment in h-i (N=6 experiments, 4-15 animals per experiment). Horizontal lines indicate mean \pm s.e.m. Data labelled with different letters indicate significant differences ($p < 0.05$, two-way ANOVA and Tukey's Post-hoc test).

observed an increase in average pause length when ADL was activated (Fig. 4h-i). From these data, we conclude that ADL mediates the increase in average pause length seen on DEET-agar, and speculate that the increase in long pauses is one mechanism by which DEET interferes with chemotaxis.

In this study, we add the nematode *C. elegans* to known DEET-sensitive animals, uncover a new neuronal mechanism for a DEET-induced behaviour, and identify a molecular target that is required for complete DEET-sensitivity in an engineered mutant and in a wild-isolate of *C. elegans*. This work opens up *C. elegans* as a system to test new repellents *in vivo* for both interference in chemotaxis and toxicity, and also for discovery of additional genes and neurons that respond to DEET. The molecular mechanism by which the *str-217* mutation renders ADL DEET-insensitive and worms DEET-resistant remains to be understood. *str-217* is a G protein-coupled receptor with no known ligand and that is evolutionarily unrelated to DEET-sensitive odorant receptor proteins previously described in insects. Although we found no evidence that DEET can activate *str-217* in heterologous cells, it is conceivable that in the right milieu that *str-217* is indeed a DEET receptor. Alternatively, *str-217* could act indirectly in concert with an as-yet unknown DEET receptor in ADL. Interestingly, pyrazine chemotaxis is unaffected by DEET in any of our assays, consistent with our model that DEET is not a simple repellent, but a modulator of pausing behaviour to interfere with chemotaxis to some but not all odorants.

These results are reminiscent of the “confusant” hypothesis in insects, although the molecular and neuronal details by which DEET acts differ markedly between species. In insects, DEET alters responses of individual sensory neurons to attractive odorants^{9,12}, thereby interfering with behavioural attraction. Our data in *C. elegans* are consistent with a mechanism where DEET can inhibit responses to some stimuli but not others by decreasing

avoidance of 2-nonanone, decreasing attractiveness to multiple odorants, and leaving pyrazine behavioural responses intact. We speculate that its promiscuity in interacting with multiple molecules and chemosensory neurons across vast evolutionary scales is the key to the broad effectiveness of DEET.

Methods

Nematode culture and strains. *C. elegans* strains were maintained at room temperature (22-24°C) on nematode growth medium (NGM) plates (51.3 mM NaCl, 1.7% agar, 0.25% peptone, 1 mM CaCl₂, 12.9 µM cholesterol, 1mM MgSO₄, 25mM KPO₄, pH 6) seeded with *Escherichia coli* (OP50 strain) bacteria as a food source^{30,31}. Bristol N2 was used as the wild-type strain. The CB4856 (Hawaiian) strain, harbouring WBVar02076179 (*str-217^{HW}*) (<http://www.wormbase.org/db/get?name=WBVar02076179;class=variation>) and Hawaiian recombinant inbred strains for chromosome V were previously generated²⁵. Generation of extra-chromosomal array transgenes was carried out using standard procedures³², and included the transgene injected at 50 ng/mL, the fluorescent co-injection marker *Pelt-2::GFP* at 5 ng/ml (with the exception of LBV004 and LBV009, which did not include a co-injection marker), and an empty vector for a total DNA concentration of 100 ng/ml. CRISPR-Cas9-mediated mutagenesis of *str-217* was performed as described, using *rol-6* as a co-CRISPR marker³³. The resulting *str-217* mutant strain [LBV004 *str-217(ejd001)*] results in a predicted frame-shift in the first exon [indel: insertion (AAAAAAA), deletion (CTGCTCCA), final sequence GCGTCGAAAAAAAATTTTCAG; insertion is underlined]. The *str-217* rescue construct (*Pstr-217::SL2::GFP*) used a 1112 nucleotide length fragment 56 nucleotides upstream 5' of the translation start of *str-217*.

Microscopy and image analysis. L2-adult stage hermaphrodites were mounted on 1% agarose pads with 10

mM sodium azide (CID 6331859, Sigma-Aldrich, catalogue #S2002) in M9 solution (22 mM KH_2PO_4 , 42mM Na_2HPO_4 , 85.6 mM NaCl, 1mM MgSO_4 , pH 6). Images were acquired with an Axio Observer Z1 LSM 780 with Apotome a 63X objective (Zeiss), and were processed using ImageJ.

Chemotaxis assays. Chemotaxis was tested as described¹⁷, on square plates containing 10 mL of chemotaxis agar (1.6% agar in chemotaxis buffer: 5 mM phosphate buffer pH 6.0, 1 mM CaCl_2 , 1 mM MgSO_4)³⁴. Additions of either ethanol (solvent-agar) or 50% DEET (CID: 4284, Sigma-Aldrich, catalogue #D100951) in ethanol (DEET-agar) were added after agar cooled to <44°C and just before pouring. A total volume of 300 μL ethanol or DEET in ethanol was added to each 100 mL of agar mixture for all experiments except **Figure 1b-c** and **Figure 4h-i**. Plates were poured on the day of each experiment, and dried with lids off for 4 hours prior to the start of the assay. 1 ml 1 M sodium azide was added to two spots on either side of the plate just before beginning the experiment to immobilize animals that reached the odorant or ethanol sources. Three days prior to all chemotaxis experiments, 4-6 L4 animals were transferred onto NGM plates seeded with *E. coli* (OP50 strain). The offspring of these 4-6 animals were then washed off of the plates and washed twice with S-Basal buffer (1 mM NaCl, 5.74 mM K_2HPO_4 , 7.35 mM KH_2PO_4 , 5 $\mu\text{g}/\text{mL}$ cholesterol at pH 6-6.2)³⁰ to remove younger animals, and once with chemotaxis buffer. Immediately before the start of the experiment, two 1 l drops of odorant diluted in ethanol, or ethanol solvent control, were spotted on each side of the plate on top of the sodium azide spots. 100-300 animals were then placed into the centre of the plate in a small bubble of liquid. The excess liquid surrounding the animals was then removed using a Kimwipe. Odorants diluted in ethanol were used in this study: 1:1000 isoamyl alcohol (CID: 31260, Sigma-Aldrich, catalogue #W205702), 1:1000 butanone (CID: 6569, Sigma-Aldrich, cata-

logue #360473), 10mg/ μL pyrazine (CID: 9261, Sigma-Aldrich, catalogue #W401501), 1:10 2-nonanone (CID: 13187, Sigma-Aldrich, catalogue #W2787513). Assays were carried out for 60-90 min at room temperature (22-24°C) between 1pm – 8pm EST. Plates were scored as soon as possible, either immediately or, if a large number of plates was being scored on the same day, plates were moved to 4°C to immobilize animals until they could be scored. The assay was quantified by counting animals that had left the origin in the centre of the plate, moving to either side of the plate (#Odorant, #Control) or just above or below the origin (#Other), and calculating a chemotaxis index as $[\# \text{Odorant} - \# \text{Control}] / [\# \text{Odorant} + \# \text{Control} + \# \text{Other}]$. A trial was discarded if fewer than 50 animals or more than 250 animals contributed to the chemotaxis index and participated in the assay.

Mutant screen. About 100 wild-type (Bristol N2) L4 animals were mutagenized in M9 solution with 50 mM ethyl methanesulfonate (CID: 6113, Sigma-Aldrich, catalogue #M0880) for 4 hours with rotation at room temperature. Mutagenized animals were picked to separate 9 cm NGM agar plates seeded with *E. coli* (OP50 strain) and cultivated at 20°C. ~5,000 F2 animals were screened for DEET resistance on 20.3 cm casserole dishes (ASIN B000LNS4NQ, model number 81932OBL11). Five animals across three assays were more than ~2 cm closer to the odour source than the rest of the animals on the plate and were defined as DEET-resistant. This phenotype was heritable in three strains, and each strain was backcrossed to OS1917 for 4 generations. Whole-genome sequencing was used to map the mutations to regions containing transversions presumably introduced by the EMS, parental alleles of the N2 strain used for mutagenesis, and missing alleles of the wild-type strain OS1917 used for backcrossing^{35,36}. LBV003 mapped to a 5 Mb region on chromosome V, that was further mapped to *str-217*. LBV002 mapped to a 6.8 Mb region on chromosome V, which was further narrowed down to a likely

candidate gene, *nstp-3(ejd002)*. In LBV002, *nstp-3(ejd002)* contains a T>G transversion of the 141st nucleotide in the CDS, which is predicted to produce a Phe48Val substitution in this sugar:proton symporter. We were unable to map the DEET-resistant mutation(s) in LBV001.

***str-217* heterologous expression.** HEK-293T cells were maintained using standard protocols in a Thermo Scientific FORMA Series II water-jacketed CO₂ incubator. Cells were transiently transfected with 1 µg each of pME18s plasmid expressing *GCaMP6s*, *Gq_α15*, and *str-217* using Lipofectamine 2000 (CID: 100984821, Invitrogen, catalogue #1168019). Control cells excluded *str-217*, but were transfected with the other two plasmids. Transfected cells were seeded into 384 well plates at a density of 2 x 10⁶ cells/ml, and incubated overnight in FluoroBrite DMEM media (ThermoFisher Scientific) supplemented with foetal bovine serum (Invitrogen, catalogue #10082139) at 37°C and 5% CO₂. Cells were imaged in reading buffer [Hanks's Balanced Salt Solution (GIBCO) + 20 mM HEPES (Sigma-Aldrich)] using GFP-channel fluorescence of a Hamamatsu FDSS-6000 kinetic plate reader at The Rockefeller University High-Throughput Screening Resource Centre. DEET was prepared at 3X final concentration in reading buffer in a 384-well plate (Greiner Bio-one) from a 46% (2 M) stock solution in DMSO (Sigma-Aldrich). Plates were imaged every 1 sec for 5 min. 10 µl of DEET solution in reading buffer or vehicle (reading buffer + DMSO) was added to each well containing cells in 20 µl of media after 30 sec of baseline fluorescence recording. The final concentration of vehicle DMSO was matched to the DEET additions, with a maximum DMSO concentration of 7.8%. Fluorescence was normalized to baseline, and responses were calculated as max ratio (maximum fluorescence level/baseline fluorescence level).

ADL calcium imaging. Calcium imaging and data analysis were performed as described³⁷, using single young adult hermaphrodites immobilized in a custom-fabricated 3 x 3 x 3 mm polydimethylsiloxane (PDMS) imaging chip.

GCaMP5k was expressed in ADL neurons under control of the *sre-1* promoter²⁷ and was crossed into *str-217*^{-/-} and the *str-217*^{-/-} rescue strain. Animals were acclimated to the imaging room overnight on *E. coli* (OP50 strain) seeded plates. All stimuli were prepared the day of each experiment, and were diluted in ethanol to 1000X the desired concentration before being further diluted 1:1000 in S-Basal buffer. Young adult animals were paralyzed briefly in (-)-tetramisole hydrochloride (CID: 27944, Sigma-Aldrich, catalogue #L9756) at 1 mM for 2-5 min before transfer into the chip to paralyze body wall muscles to keep animals stationary during imaging. All animals were pre-exposed to light (470+/- 40nm) for 100 sec before recording to attenuate the light response of ADL³⁸. Experiments consisted of the following stimulation protocol: 20 sec S-Basal buffer, followed by 3 repetitions of 20 sec DEET (0.15% DEET and 0.15% ethanol in S-Basal) and then 20 sec S-basal buffer.

GCaMP signals were recorded with Metamorph Software (Molecular Devices) and an iXon3 DU-897 EMCCD camera (Andor) at 10 frames/sec using a 40x objective on an upright Zeiss Axioskop 2 microscope. Custom ImageJ scripts¹⁷ were used to track cells and quantify fluorescence. In **Figure 3d** and **f**, all frames in 20 sec before the DEET pulse were averaged and subtracted from the average of the frames during the 20 sec DEET or C9 pulse to calculate ΔF . In **Figure 3e** and **g**, traces were bleach corrected using a custom MATLAB script and then the 5% of frames with the lowest values were averaged to create F_0 . $\Delta F/F_0$ was calculated by $(F - F_0)/F_0$ and then divided by the maximum value to obtain $\Delta F/F_{\max}$ ³⁹. The heatmap traces in **Figure 3e** and **g** were also smoothed by 5 frames, such that each data point n is the running average of $n-2$, $n-1$, n , $n+1$, and $n+2$.

AWC calcium imaging. Calcium imaging of freely moving worms and subsequent data analysis were performed as described³⁹, using a 3 mm² microfluidic PDMS device with two arenas that enabled simultaneous imaging of two genotypes with approximately 10 animals each. We used an integrated line (CX17256) expressing GCaMP5a in AWC^{ON}

neurons under control of the *str-2* promoter crossed into *str-217^{-/-}* animals. Adult hermaphrodites were first paralyzed for 80-100 min in 1 mM (-)-tetramisole hydrochloride and then transferred to the arenas in S-Basal buffer. The stimulus protocol was as follows: In S-Basal, three pulses of 60 sec in buffer and 30 sec isoamyl alcohol, followed by 120 sec in buffer. Next, the animals were switched to S-Basal with 0.15% ethanol (solvent buffer) and three pulses of 60 sec in buffer and 30 sec in isoamyl alcohol in solvent buffer followed by 120 sec in solvent buffer before a switch to S-Basal with 0.15% ethanol and 0.15% DEET (DEET buffer). In DEET buffer, animals were given 6 pulses of 60 sec in DEET buffer and then 30 sec in isoamyl alcohol in DEET buffer, followed by 120 sec in DEET buffer before switching to solvent buffer. In solvent buffer, the animals received three pulses of 60 sec in buffer and 30 sec in isoamyl alcohol in solvent buffer followed by 120 sec in solvent buffer before a switch to S-Basal. In S-Basal, the animals received three pulses of 60 sec in buffer and 30 sec isoamyl alcohol, followed by 60 sec in buffer.

Each experiment was repeated 3-4 times over 2-3 days and pooled by strain for analysis (wild-type: 31 animals, 4 experiments, 3 days; *str-217^{-/-}*: 23 animals, 3 experiments, 2 days). Images were acquired at 10 frames/sec at 5X magnification (Hamamatsu Orca Flash 4 sCMOS), with 10 msec pulsed illumination every 100 msec (Sola, Lumencor; 470/40 nm excitation). Fluorescence levels were analysed using a custom ImageJ script that integrates and background-subtracts fluorescence levels of the AWC neuron cell body (6×6 pixel region of interest). Traces were normalized by subtracting and then dividing by the baseline fluorescence, defined as the average fluorescence of the last 2 sec of the first three isoamyl alcohol pulses. The traces in **Extended Data Figure 1** were also smoothed by 5 frames, such that each data point n is the running average of $n-2$, $n-1$, n , $n+1$, and $n+2$. The response magnitudes were calculated by taking the mean of the last 2 sec of an isoamyl alcohol pulse, subtracting the mean of the 2 sec before the isoamyl alcohol pulse (F0), and dividing by this

F0. The response magnitudes were calculated for the 5th (0.15% ethanol in S-Basal buffer), 8th (0.15% DEET and 0.15% ethanol in S-Basal buffer), and 14th (0.15% ethanol in S-Basal buffer) isoamyl alcohol pulses. We also quantified the response magnitude of the transition from S-Basal buffer with ethanol to S-Basal buffer with DEET. We took the mean of the first 2 sec after switching to DEET buffer, subtracted the mean of the 2 sec before switching (F0), and divided by this F0.

Chemotaxis tracking and analysis. 8-20 adult hermaphrodites were first transferred to an empty NGM plate and then 4-15 were transferred to an assay plate to minimize bacterial transfer. Animals were then placed in the centre on either a 0.15% DEET-agar or solvent-agar plate, and their movement was recorded for 60 min at 3 frames/sec with 6.6 MP PL-B781F CMOS camera (PixeLINK) and Streampix software. Assays were carried out at room temperature, between 12-8pm EST, and lit from below. Worm trajectories were extracted by a custom Matlab (MathWorks) script¹⁷, and discontinuous tracks were then manually linked. Tracks were discarded if the animal moved less than two body lengths from its origin over the course of the 60 min trial. If an animal came within 1cm of the isoamyl alcohol stimulus, the track was truncated to remove information from animals immobilized at the odour source because of the addition of sodium azide.

ADL optogenetic stimulation. L4 animals expressing an *Psrh-220::ReaChR²⁹* array or array-negative animals from the same plate were raised overnight in the dark on an NGM plate freshly seeded with 100 μ L of 10X concentrated *E. coli* (OP50 strain) with or without 50 μ M all-*trans* retinal (CID: 720648, Sigma-Aldrich, catalogue #R2500), which is required for ReaChR-induced activity. The next day, adult hermaphrodites were first transferred to an empty NGM plate and then 4-15 animals were transferred to the 10 cm circular assay plate to minimize bacterial transfer. Videos were recorded for 26 min at 3 frames/sec with a 1.3 MP PL-A741 camera (PixeLINK) and Streampix

software. Blue light pulses were delivered with an LED (455 nm, 20 μ W/mm², Mightex) controlled with a custom Matlab script^{17,40}. Animals were exposed to normal light for 120 sec, before exposure to 12 pulses of blue light (455 nm, 10 Hz strobing) for 120 sec, followed by 120 sec of recovery. This should activate ADL neurons only in retinal-fed animals expressing ReaChR. Worm trajectories were extracted by a custom Matlab script⁴⁰. Pausing events were extracted, and all pauses ≥ 3 frames (1 sec) were used for further analysis. Pauses were classified as “ON” if any frame included light illumination. A pause that began just before illumination began, but remained paused while the illumination occurred, was considered an ON pause, just as a pause that occurred in the middle of a light illumination time frame was considered ON. All other pauses were classified as “OFF” pauses. In the analysis in Figure 4h, we took an average pause length for all ON pauses and all OFF pauses for each animal, and pooled all of the animals on each plate. To control for any baseline differences between animals and experiment-to-experiment variation, we examined the increase in average pause length in Figure 4i.

Statistical Analysis. R v3.3.2 was used for all statistical analysis. Inclusion and exclusion criteria were pre-established for all experiments, and in behaviour experiments positions were pseudo-randomized. All scripts and raw data with the exception of raw video files are available in Supplemental Data File 1. Scripts to analyse these data are also available at this link: http://github.com/VosshallLab/Dennis-Emily_2017

Strains. Detailed genotypes of all *C. elegans* strains and their sources^{25,28,29,38,41-43} are in Extended Data Table 1.

References

- 1 Travis, B. V., Morton, F. A. & et al. The more effective mosquito repellents tested at the Orlando, Fla., laboratory, 1942-47. *J Econ Entomol* **42**, 686-694 (1949).
- 2 McCabe, E. T., Barthel, W. F., Gertler, S. I. & Hall, S. A. Insect Repellents. III. N, N-diethylamides. *J. Org. Chem.* **19**, 493-498 (1954).
- 3 Katz, T. M., Miller, J. H. & Hebert, A. A. Insect repellents: historical perspectives and new developments. *J Am Acad Dermatol* **58**, 865-871 (2008).
- 4 Tawatsin, A. *et al.* Field evaluation of deet, Repel Care, and three plant based essential oil repellents against mosquitoes, black flies (Diptera: Simuliidae) and land leeches (Arhynchobdellida: Haemadipsidae) in Thailand. *J Am Mosq Control Assoc* **22**, 306-313 (2006).
- 5 Abramson, C. I. *et al.* Proboscis conditioning experiments with honeybees, *Apis mellifera caucasica*, with butyric acid and DEET mixture as conditioned and unconditioned stimuli. *J Insect Sci* **10**, 122 (2010).
- 6 Carroll, J. F., Klun, J. A. & Debboun, M. Repellency of deet and SS220 applied to skin involves olfactory sensing by two species of ticks. *Med Vet Entomol* **19**, 101-106 (2005).
- 7 Nath, D. R., Das, N. G. & Das, S. C. Bio-repellents for land leeches. *Def. Sci. J.* **52**, 72 (2002).
- 8 Dogan, E. B., Ayres, J. W. & Rossignol, P. A. Behavioural mode of action of deet: inhibition of lactic acid attraction. *Med Vet Entomol* **13**, 97-100 (1999).
- 9 Ditzen, M., Pellegrino, M. & Vosshall, L. B. Insect odorant receptors are molecular targets of the insect repellent DEET. *Science* **319**, 1838-1842 (2008).
- 10 Syed, Z. & Leal, W. S. Mosquitoes smell and avoid the insect repellent DEET. *Proc Natl Acad Sci U S A* **105**, 13598-13603 (2008).
- 11 Liu, C. *et al.* Distinct olfactory signaling mechanisms in the malaria vector mosquito *Anopheles gambiae*. *PLoS Biol* **8** (2010).
- 12 Pellegrino, M., Steinbach, N., Stensmyr, M. C., Hansson, B. S. & Vosshall, L. B. A natural polymorphism alters odour and DEET sensitivity in an insect odorant receptor. *Nature* **478**, 511-514 (2011).
- 13 DeGennaro, M. *et al.* *orco* mutant mosquitoes lose strong preference for humans and are not repelled by volatile DEET. *Nature* **498**, 487-491 (2013).

- 14 Xu, P., Choo, Y. M., De La Rosa, A. & Leal, W. S. Mosquito odorant receptor for DEET and methyl jasmonate. *Proc Natl Acad Sci U S A* **111**, 16592-16597 (2014).
- 15 Bargmann, C. I. & Horvitz, H. R. Chemosensory neurons with overlapping functions direct chemotaxis to multiple chemicals in *C. elegans*. *Neuron* **7**, 729-742 (1991).
- 16 Troemel, E. R., Kimmel, B. E. & Bargmann, C. I. Reprogramming chemotaxis responses: sensory neurons define olfactory preferences in *C. elegans*. *Cell* **91**, 161-169 (1997).
- 17 Cho, C. E., Brueggemann, C., L'Etoile, N. D. & Bargmann, C. I. Parallel encoding of sensory history and behavioral preference during *Caenorhabditis elegans* olfactory learning. *Elife* **5** (2016).
- 18 Syed, Z., Pelletier, J., Flounders, E., Chitolina, R. F. & Leal, W. S. Generic insect repellent detector from the fruit fly *Drosophila melanogaster*. *PLoS One* **6**, e17705 (2011).
- 19 Bargmann, C. I., Hartweg, E. & Horvitz, H. R. Odorant-selective genes and neurons mediate olfaction in *C. elegans*. *Cell* **74**, 515-527 (1993).
- 20 Reeder, N. L., Ganz, P. J., Carlson, J. R. & Saunders, C. W. Isolation of a deet-insensitive mutant of *Drosophila melanogaster* (Diptera: Drosophilidae). *J Econ Entomol* **94**, 1584-1588 (2001).
- 21 Stanczyk, N. M., Brookfield, J. F., Ignell, R., Logan, J. G. & Field, L. M. Behavioral insensitivity to DEET in *Aedes aegypti* is a genetically determined trait residing in changes in sensillum function. *Proc Natl Acad Sci U S A* **107**, 8575-8580 (2010).
- 22 Robertson, H. M., Warr, C. G. & Carlson, J. R. Molecular evolution of the insect chemoreceptor gene superfamily in *Drosophila melanogaster*. *Proc Natl Acad Sci U S A* **100 Suppl 2**, 14537-14542 (2003).
- 23 Missbach, C. *et al.* Evolution of insect olfactory receptors. *Elife* **3**, e02115, doi:10.7554/eLife.02115 (2014).
- 24 Sarin, S. *et al.* Analysis of multiple ethyl methanesulfonate-mutagenized *Caenorhabditis elegans* strains by whole-genome sequencing. *Genetics* **185**, 417-430 (2010).
- 25 Doroszuk, A., Snoek, L. B., Fradin, E., Riksen, J. & Kammenga, J. A genome-wide library of CB4856/N2 introgression lines of *Caenorhabditis elegans*. *Nucleic Acids Res* **37**, e110 (2009).
- 26 Zaslaver, A. *et al.* Hierarchical sparse coding in the sensory system of *Caenorhabditis elegans*. *Proc Natl Acad Sci U S A* **112**, 1185-1189 (2015).
- 27 Jang, H. *et al.* Neuromodulatory state and sex specify alternative behaviors through antagonistic synaptic pathways in *C. elegans*. *Neuron* **75**, 585-592 (2012).
- 28 Schiavo, G. *et al.* Tetanus toxin is a zinc protein and its inhibition of neurotransmitter release and protease activity depend on zinc. *Embo j* **11**, 3577-3583 (1992).
- 29 Lin, J. Y., Knutsen, P. M., Muller, A., Kleinfeld, D. & Tsien, R. Y. ReaChR: a red-shifted variant of channelrhodopsin enables deep transcranial optogenetic excitation. *Nat Neurosci* **16**, 1499-1508 (2013).
- 30 Brenner, S. The genetics of *Caenorhabditis elegans*. *Genetics* **77**, 71-94 (1974).
- 31 Stiernagle, T. Maintenance of *C. elegans*. WormBook, ed. The *C. elegans* Research Community, WormBook, doi:10.1895/wormbook.1.101.1 (2006). <http://wormbook.org>
- 32 Mello, C. & Fire, A. DNA transformation. *Methods Cell Biol* **48**, 451-482 (1995).
- 33 Arribere, J. A. *et al.* Efficient marker-free recovery of custom genetic modifications with CRISPR/Cas9 in *Caenorhabditis elegans*. *Genetics* **198**, 837-846 (2014).
- 34 Hart, A. C., ed. Behavior (July 3, 2006), WormBook, ed. The *C. elegans* Research Community, WormBook, doi:10.1895/wormbook.1.87.1, <http://www.wormbook.org>.
- 35 Zuryn, S., Le Gras, S., Jamet, K. & Jarriault, S. A strategy for direct mapping and identification of mutations by whole-genome sequencing. *Genetics* **186**, 427-430 (2010).
- 36 Kutscher, L. M. & Shaham, S. Forward and reverse mutagenesis in *C. elegans*. WormBook, ed. The

C. Elegans Research Community, WormBook, doi:10.1895/wormbook.1.167.1 (2014). <http://www.wormbook.org>.

- 37 Larsch, J. *et al.* A circuit for gradient climbing in *C. elegans* chemotaxis. *Cell Rep* **12**, 1748-1760 (2015).
- 38 Jang, H. *et al.* Dissection of neuronal gap junction circuits that regulate social behavior in *Caenorhabditis elegans*. *Proc Natl Acad Sci U S A* **114**, E1263-e1272 (2017).
- 39 Larsch, J., Ventimiglia, D., Bargmann, C. I. & Albrecht, D. R. High-throughput imaging of neuronal activity in *Caenorhabditis elegans*. *Proc Natl Acad Sci U S A* **110**, E4266-4273 (2013).
- 40 Gordus, A., Pokala, N., Levy, S., Flavell, S. W. & Bargmann, C. I. Feedback from network states generates variability in a probabilistic olfactory circuit. *Cell* **161**, 215-227 (2015).
- 41 Fatt, H. V. & Dougherty, E. C. Genetic control of differential heat tolerance in two strains of the nematode *Caenorhabditis elegans*. *Science* **141**, 266-267 (1963).
- 42 Hodgkin, J. & Doniach, T. Natural variation and copulatory plug formation in *Caenorhabditis elegans*. *Genetics* **146**, 149-164 (1997).
- 43 Yoshimura, S., Murray, J. I., Lu, Y., Waterston, R. H. & Shaham, S. *mls-2* and *vab-3* control glia development, *hlh-17/Olig* expression and glia-dependent neurite extension in *C. elegans*. *Development* **135**, 2263-2275 (2008).

Acknowledgements

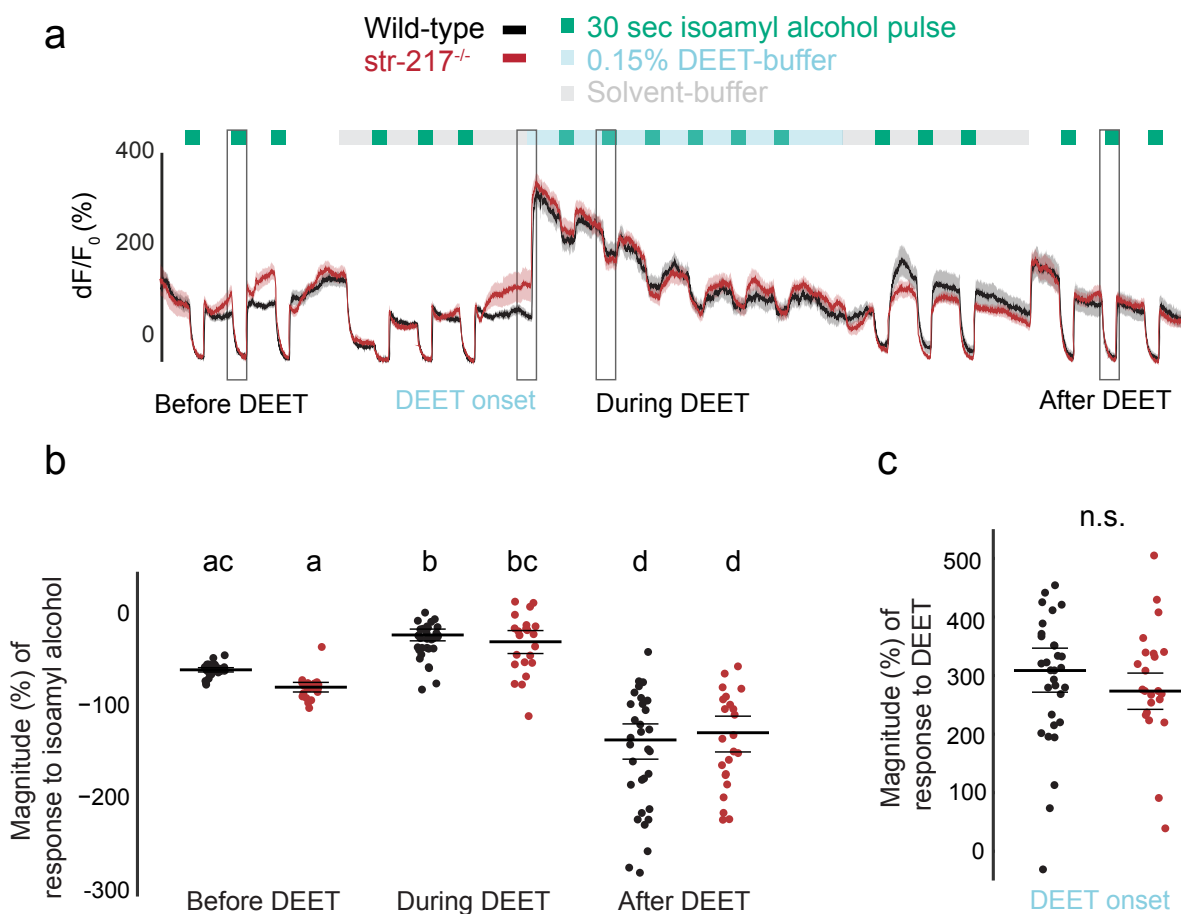
We thank Michael Crickmore, Kevin Lee, Aakanksha Singhvi, Nilay Yapici, and members of the Voshall Lab for discussion and comments on the manuscript. Shai Shaham advised and Wendy Wang assisted with chemical mutagenesis. Heeun Jang provided guidance on chemotaxis behaviour and imaging. Alejandro Lopez-Cruz and Elias Sheer provided advice on tracking behaviour. Sagi Levy shared the *Pstr-2::GCaMP5a* strain and Elias Sheer shared the *Psrh-220::ReaChR* plasmid. We thank Anh Nguyen for

her contributions to the early analysis of DEET-resistant mutants in the Hartman laboratory. Some *C. elegans* strains used in this paper were obtained from the CGC, which is funded by NIH Office of Research Infrastructure Programs (P40 OD010440). This work was supported by an NIH grant to E.J.D. (F31 DC014222). L.B.V. is an investigator of the Howard Hughes Medical Institute.

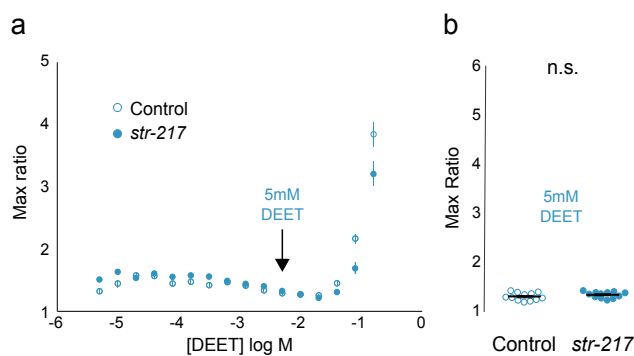
Author Contributions E.J.D. and L.B.V. developed the concept and designed the experiments. E.J.D. performed all experiments and analysis unless noted. X.J. carried out imaging experiments in Figure 3 along with E.J.D., and performed cell identification. M.D. performed AWC calcium-imaging experiments in Extended Data Figure 1. L.B.D. performed HEK cell experiments in Extended Data Figure 2. C.I.B. provided guidance, reagents, experimental design advice, identified cells, and interpreted data. P.S.H. made the original observation that DEET interferes with chemotaxis in *C. elegans*, and initiated genetic screens for DEET-resistant mutants in his laboratory. E.J.D. and L.B.V. together interpreted the results, designed the figures, and wrote the paper with input from the other authors. The authors declare no competing financial interests.

Extended Data Table 1| Detailed strain list

Text name	Strain name	Genotype	AddGene plasmid	References	Notes	Appears in:
Wild-type	N2 (Bristol)	Wild-type	N/A	[41]	N/A	Figures 1, 2, 3, 4
LBV001	LBV001	Unknown	N/A	This paper	EMS screen, backcrossed 4x	Referenced in text
LBV002	LBV002	<i>nstp-3(ejd002[F48V])</i>	N/A	This paper	EMS screen, backcrossed 4x	Referenced in text
LBV003	LBV003	<i>str-217(ejd003[P314S])</i>	N/A	This paper	EMS screen, backcrossed 4x	Figure 1h and Figure 2d
LBV003 rescue	LBV004	<i>str-217(ejd003); ejdEx1[pLV001(Pstr-217::str-217::SL2::GFP)]</i>	pLV001	This paper	N/A	Figure 2d
ewlR73	ewlR73	<i>str-217(N2)</i>	N/A	[25]	chrV:~14.0-17.4 Mb CB4856>N2	Figure 2b
ewlR74	ewlR74	<i>str-217(WBVar02076179)</i>	N/A	[25]	chrV:~14.0-18.6 Mb CB4856>N2	Figure 2b-c
ewlR74 rescue	LBV009	<i>str-217(WBVar02076179); ejdEx1[pLV001(Pstr-217::str-217::SL2::GFP)]</i>	pLV001	[25] and this paper	N/A	Figure 2c
ewlR76	ewlR76	<i>str-217(N2)</i>	N/A	[25]	chrV:~17.4-21 Mb CB4856>N2	Figure 2b
Hawaiian	CB4856	Hawaiian strain	N/A	[42]	N/A	Figure 2b
str-217-/-	LBV005	<i>str-217(ejd001)</i>	(pJA42, pDD162, pLV002)	This paper	CRISPR-Cas9-induced lesion	Figure 2d, 3b-f, 4d and e
str-217-/- rescue	LBV006	<i>str-217(ejd001); ejdEx2[pLV002(Psrh-220::str-217::mCherry)]</i>	pLV003	This paper	N/A	Figure 2d, 3b-f
ADL::TeTX	CX12328	<i>kyEx3438[Psre-1(1kb)::TeTX::SL2::mCherry + coel::DsRed]</i>	N/A	[28]	N/A	Figure 3b, 4f
ADL::ReaChR	LBV007	<i>ejdEx3[pES01(Psrh-220::ReaChR)]</i>	N/A	[29]	Plasmid from the Bargmann lab	Figure 4h-l
ADL::GCaMP	CX16616	<i>mzmEx[Psre1::GCaMP5kopt + Psre-1::tagRFP]</i>	N/A	[38]	N/A	Figure 3 c-f
mutant ADL::GCaMP	LBV008	<i>str-217(ejd001);mzmEx[Psre1::GCaMP5kopt + Psre-1::tagRFP]</i>	N/A	[38] and this paper	N/A	Figure 3c-f
rescue ADL::GCaMP	LBV009	<i>str-217(ejd001); mzmEx[Psre1::GCaMP5kopt + Psre-1::tagRFP]]]; ejdEx2[Psrh-220::str-217::mCherry]</i>	pLV003	[38] and this paper	N/A	Figure 3 c-f
AWC::GCaMP	CX17256	<i>kyls722[Pstr-2::GCaMP5a]</i>	N/A	this paper	Plasmid from Sagi Levy (Bargmann Lab) integrated by UV, backcrossed 4x to N2	Extended Data Figure 2
str-217-/-; AWC::GCaMP	LBV010	<i>str-217(ejd001);kyls722[Pstr-2::GCaMP5a]</i>	N/A	this paper	N/A	Extended Data Figure 2
Pptr10::myrRFP	OS1907	<i>nsIs108(Pptr-10::myrRFP)</i>	N/A	[43]	Gift from the Shaham lab	Referenced in text



Extended Data Figure 1 | $str-217$ -independent responses of chemosensory neuron AWC^{ON} to DEET. **a**, Top: stimulus protocol. 30 sec pulses of isoamyl alcohol (dark grey) were delivered in buffer, buffer with solvent (light grey), or buffer with 0.15% DEET (blue). Bottom: Average traces of GCaMP activity in AWC^{ON} in wild-type (black) and $str-217^{-/-}$ (red) animals over a 36 min experiment, used for analysis in **b** and **c**. **b**, Response magnitudes of the isoamyl alcohol response before, during, and after DEET. **c**, Response magnitude of the increase in calcium in AWC at DEET onset (N=23 $str-217$, N=31 wild-type animals in 3-4 experiments over 2-3 days). In **b** and **c**, each dot represents responses of single animals and the horizontal lines represent the mean and s.e.m. Data labelled with different letters indicate significant differences ($p < 0.05$, two-way ANOVA and Tukey's Post-hoc test in **b**, and two-tailed Student's t-test in **c**).



Extended Data Figure 2 | $str-217$ does not respond to DEET when expressed in HEK-293T cells. **a**, Max ratio (maximum fluorescence/baseline fluorescence) of calcium signal in HEK-293T cells transiently expressing GCaMP6s and $Gq_{\alpha}15$ without (control) or with $str-217$ and stimulated by the indicated dose of DEET. **b**, Summary of max ratio responses to 5 mM DEET. Data are plotted as mean \pm s.e.m. (n=12, 3 replicates each in 4 separate plates; n.s., not significant, $p > 0.05$, ANOVA and Tukey's Post-hoc test) with s.e.m. indicated by a vertical line in **a** and horizontal line in **b**.